

REPORT ON BSEE CONTRACT NO. E14PC00008

DEVELOPMENT OF HAZARD CURVES FOR WEAS OFF THE ATLANTIC SEABOARD

Dr. Paul T. Gayes¹

Dr. Leonard J. Pietrafesa¹

Dr. Shaowu Bao¹

Dr. Tingzhuang Yan¹

Dr. Turel Gur²

¹Coastal Carolina University

²MMI Engineering

December 2, 2015

Executive summary	3
1. Introduction	5
1.1. Background	5
1.2. Technical Approach	5
2. Selection of Wind Farm Sites and Storm Database	6
2.1. Selection of Sites	6
2.2. Identification of Storms	7
3. Hindcast Case Studies and Verification	8
3.1. Summary of Hindcast and Verification.	8
3.2. Overview of methods	8
3.3. Selection of Storms for Case Studies	10
3.4. Model Results and Verification	10
4. Storm Hindcast and Development of Metocean Hazard Curves	14
5. Supplemental Extra-Tropical Storm Database	20
5.1. Curves for ETC+TC cases	20
5.2. Curves for ETC-only cases	22
6. Load Factor Calibration Study	24
6.1. Wind and Wave Exceedance Curves	24
6.2. Approach	27
6.3. Mudline OTM Exceedance Curves	29
6.4. Calculation of Load Factors for Tropical Cyclones	33
6.5. Discussion of Results	37
Appendix A buoy stations and storm tracks	38
Appendix B. Acronyms	39

Executive summary

1. The CCU and MMI teams worked together to select and study seven (initially there were five BOEM sites, but later BOEM increased that to seven) regions along the United States (U.S.) Atlantic Eastern Seaboard. These selected study sites are deemed to be representative of the sites identified by BOEM for wind farm development auctions and include several sites that may also be considered by BOEM for future development. Most of the seven selected regions have both shallow water and deep-water locations as parts of their extended domains (Figure 1).
2. The International Best Track Archive for Climate Stewardship (IBTrACS), which includes Tropical Cyclone (TC) information from 1848 to 2013, was used to identify TC storms that had extensively and intensively impacted the seven selected regions.
3. The Extra-Tropical Cyclone (ETC) data (1979-2013) from the North America Regional Reanalysis (NARR), whose data extends from 1979 to 2013, was used to identify U.S. east coast mid-latitude, extra-tropical cyclones (ETCs), also known as nor'easter winter storms that affected the seven selected regions.
4. In total, about 1500 TC and ETC storms were identified in items (2) and (3).
5. In-Situ National Oceanic & Atmospheric Administration (NOAA) - National Data Buoy Center (NDBC) Marine Buoy 10-m wind speed and significant wave height data were collected from buoys located near the seven regional locales. The NDBC buoy locations and designations are shown in Appendix A.
6. A CCU developed atmosphere-ocean-wave interactively coupled high-resolution numerical model was used to downscale and hind-cast the identified storms. Well-documented TCs and an ETCs were used to validate model hind-casted wind strength and significant wave height results against the NOAA NDBC in-situ Marine Buoy observations. The validations demonstrated reasonably good agreement.
7. Subsequent to the CCU model output validations in (6), all the identified storms were downscaled and hind-casted.
8. The wind strength and significant wave height numerical modeling results (7), extracted from the CCU hind-cast modeling, were used to develop the exceedance curves for the seven selected domains.
9. For the ETC model output data set, CCU discovered that a 1993 winter storm, which had the wind strength equivalent to a Category-2 hurricane, caused extraordinarily high waves over most of the seven selected regions due to its strong winds and affected a significantly large impact area, as it had along lasting period; and thus generated a considerable fetch. The high waves caused by this 1993 winter storm far exceeded those caused by any other ETC in the record.
10. So, in an attempt to evaluate the significance of the March 1993 event (9) in the database, CCU conducted an extensive statistical evaluation of all outlier waves observed at the NOAA NDBC Marine Buoys in the seven domains and found that this event was truly singular in its wave magnitude.
11. Because the March 1993 singular event dominated the wave height ETC exceedance curve due to the relatively short 34-year data base of ETCs, this fact caused difficulties in developing load factors from the

wind and wave exceedance curves in the subsequent tasks. It was observed that the 1993 singularly large event created a major bias in the results.

12. Here (11) there were several conference calls with BSEE, MMI and CCU representatives regarding a course of action and it was proposed to increase the data length of ETCs by including a supplement database that dates back to 1950.
13. Utilization of the extended database resulted in more regular shaped exceedance curves and load factors within ranges believed to be realistic and in line with physical conditions of the sites and gradient in storm types and intensities along the latitudinal gradient of the U.S. eastern seaboard.
14. Load factors for TCs were estimated using the exceedance curves. For Sites 1 through 6, the target return period obtained using the standard IEC load factor of 1.35 ranges between 153 years to 276 years, and the load factor estimates for TCs range between 1.37 (in the northern part of the overall eastern seaboard domain, where TCs are weaker) and 1.94 (in the southern part of the overall eastern seaboard domain, where the TCs are stronger). Site 7 has realized very few TC realizations, thus the statistics of those TC passages are very weak; therefore the load factor for TCs could not be calculated for the Maine site. These results show the relative role of TCs and ETCs along east coast with end members 1 and 7 responding to a greater proportion of TC and ETC's, respectively.

1. Introduction

The results presented in this report was performed under contract Number E14PC00008 awarded by the Bureau of Safety and Environmental Enforcement (BSEE) for support of the project entitled "Establishment of Met-ocean Data and Hazard Curves for Wind Energy Areas (WEAs) off the Atlantic Seaboard: Virginia Offshore Wind Gathering Program."

1.1. BACKGROUND

MMI Engineering (MMI) completed a Joint Industry Project (JIP) in 2008 titled "Comparative Study of Offshore Wind Turbine Generator Standards" funded by the U.S. Minerals Management Service (MMS) and the U.S. National Renewable Energy Laboratory (NREL), along with several private organizations interested in offshore wind energy systems. The objective of this study was to evaluate the comparative reliabilities of the wind turbine support structures designed per API and IEC standards for areas in the U.S. subject to hurricane conditions. A core objective of this prior study was the assessment of the effect of load uncertainty on the overall reliability of the support structure design. This study determined that the uncertainties associated with hurricane winds and waves required higher load factors to develop designs with levels of reliability consistent with those intended by either API or IEC standards.

The prior projects included case studies and detailed reliability analyses to quantify the effect of hurricane loading uncertainties using site specific data developed for two locations: offshore Massachusetts and offshore Texas. These detailed studies developed safety indices for extreme load conditions using site specific data as it is applied to indicative monopile, tripod and jacket type support structures. This work provided a starting point for the definition of load factors to address hurricane load conditions in the US; however, the limited number of case studies that were performed does not provide the basis that is necessary to cover the range of conditions that exist along the east coast. The study concluded that additional work was required to develop wind, wave and current exceedance data for the OCS areas subject to tropical storms to provide the basis to determine appropriate adjustments in load factors for support structure design.

1.2. TECHNICAL APPROACH

The approach applied in the project included two main elements. The first is the development of wind and wave exceedance data that is representative of conditions along the U.S. Eastern Atlantic Seaboard coast of the U.S. Outer Continental Shelf (OCS) where wind farms may be developed. These exceedance curves represent the uncertainties in the definition of met-ocean conditions that drive higher load factor requirements in areas subject to tropical cyclone atmospheric storms and extra-tropical cyclone atmospheric storms.

The second element of the approach is the calibration of load factors for the different regions to achieve consistent levels of structural reliability for typical support structure designs. The methodology that was developed by MMI during the prior study would be repeated for this part of the work.

This report details the study conducted by the project team for the 7 newly identified sites.

2. Selection of Wind Farm Sites and Storm Database

2.1. SELECTION OF SITES

With renewable energy on the verge of massive growth, much research emphasis is put on the selection of potential wind farm sites and analysis of metocean condition and hazard curve on those sites. Site selection method in this study is based on a spatial cost–revenue optimization with the following factors being considered:

- 1) Land use and geological constraints
- 2) Costs from access roads, power lines and land clearing.
- 3) Existing wind turbine farms.
- 4) 100-year wind segmentation of US East Coast

After evaluation of the above factors, seven potential wind farm sites have been identified (Figure 1). The Bureau of Ocean Energy Management (BOEM) has identified several blocks along the U.S. Atlantic Eastern Seaboard for the auction of wind farm developments, including those in Massachusetts, Rhode Island, New Jersey, Delaware, Maryland and Virginia. These blocks are considered in our site selection. Several of these identified sites are combined due to the proximity of their locations. Sites 1, 2, 3 and 4 shown in Figure 1 are the sites that have already been identified by BOEM for wind farm development. Besides these BOEM-identified sites, three additional sites (sites 5, 6 and 7 in Figure 1) were included in this project to represent those regions for potential future development consideration.

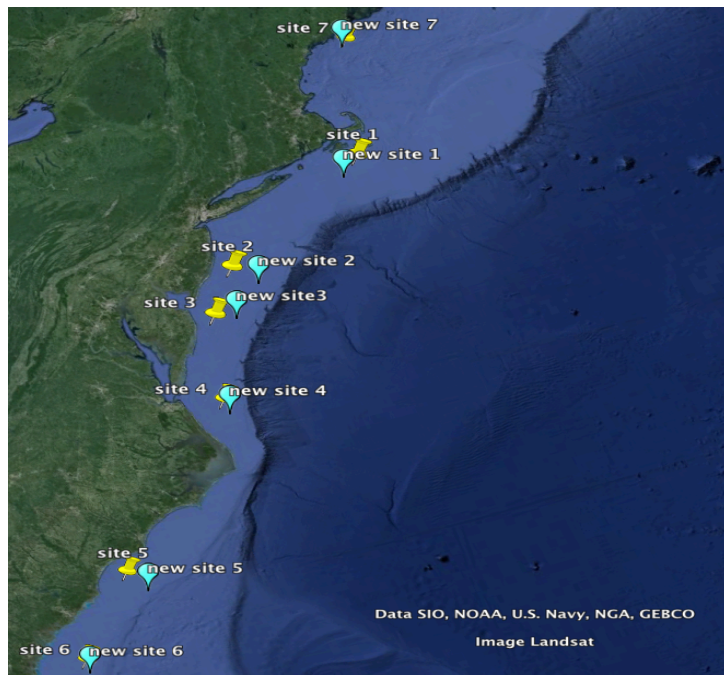


Figure 1 Selected seven potential wind farm development sites for this study.

ocean conditions.

Note that several of the selected sites have water depths that are shallow enough to affect the surface wave height due to oceanic surface gravity wave breaking processes. Therefore when the wind strength and wave height data were extracted from the model hind-cast, locations slightly different from those listed in Table 1 (shown as the cyan marks and labeled as “new site #” in Figure 1), which have deeper water depths, were used to avoid the influence of the shallow bathymetry on met-

Table 1 Latitude and Longitude for the selected farm development sites

Site	Latitude (N)	Longitude (W)
1	45°56'	70°33'
2	39°17'	74°01'
3	38°22'	74°45'
4	36°31'	75°18'
5	33°21'	78°36'
6	31°33'	80°10'
7	43°30'	69°31'

2.2. IDENTIFICATION OF STORMS

The metocean values (wind, current, wave and water level) and hazard curves (peak metocean value versus the annual exceedance probability) are described as high and low probability metocean conditions. The hazards caused by tropical cyclones (TC) and extra-tropical cyclones (ETC) both can have significant impacts on wind farm development, so analysis on the historical TCs and ETCs that have passed through or near those selected farm sites is necessary.

We have identified all the TCs archived in the International Best TRack Archive for Climate Stewardship (IBtracks) database (1851-2013) whose storm center has been observed to be within a radius of 200km to the site center. The ETCs were initially identified in the North American Regional Reanalysis (NARR) database (containing storms 1979-2013). A supplemental database, the NCAR/NCEP reanalysis (containing storms 1948-1978), was later found necessary to obtain reasonable exceedance curves.

The ETCs in the NCAR/NCEP reanalysis database were also identified and included in the study. Those storms whose maximum 10-meter wind speed within an area of 100 km X 100 km centered by the identified sites exceeded 34 kts (tropical storm strength) are selected. The identified tropical cyclones and extra-tropical cyclones are listed in (the list of storms is available at CCU or in the original format within the respective databases) and used for subsequent tasks.

3. Hindcast Case Studies and Verification

3.1. SUMMARY OF HINDCAST AND VERIFICATION.

The CCU team conducted several case studies and verified the results with available observations, thus confirmed that the modeling suite and hind-cast method proposed for this project are able to reasonably realistically represent the met-ocean conditions at the seven proposed wind farm sites caused by historical tropical cyclones (TCs) and extra-tropical cyclones (ETCs).

The 2011 TC Irene and 1993 ETC winter storm were selected for case studies. The following two methods were used to provide surface wind fields to the coupled ocean and wave models: the empirical Holland vortex method (for TC Irene) and the full-physics WRF modeling (for the 1993 ETC). The Holland method is needed in this study for those storms prior to 1948 for which there are no reanalysis data to initialize the WRF model.

Irene was simulated from 2011-08-26-00 to 2011-08-29-00. The 1993 ETC simulation was from 1993-03-13-06 to 1993-03-15-06. Observational data from all the buoy stations that are located close to the paths of these two storms and have valid data during the simulation period were used to verify the simulated wind and wave fields. The verification showed reasonably good agreement between the model simulations and buoy observations. This suggests that the production hindcast, which we conducted, which includes all the TCs and ETCs that we identified, created a dataset that reasonably and realistically represented the climatological met-ocean conditions at the seven proposed potential wind farm development sites and therefore could be used to create the exceedance curves.

3.2. OVERVIEW OF METHODS

When constructing a regional metocean data set, it is usually assumed that the past climate metocean can be projected into future conditions. For a specific wind farm site, model hindcast and observation are two main sources to obtain the past climate metocean data. Model hindcasting has become the primary method for wind turbine exceedance assessments since metocean observations have both spatial and temporal gaps, especially over and across continental margin regions, which make them less useful in hazard studies and analyses. However, although scarce, atmospheric and oceanic in-situ observational data are essential in the verification and validation of the model's hindcast capabilities.

Atmospheric and oceanic reanalysis datasets are sufficient for metocean data analysis associated with non-storm weather conditions. However for storm conditions, such as hurricanes and winter storms, the relatively coarse resolutions of the currently available reanalysis datasets can lead to unrealistic estimates of the wind, currents, wave and water level conditions, and are found to underestimate their values. The common method of generating metocean data by model hindcasting is to use atmospheric reanalysis of relatively coarse spatial resolution (typically 20-100 km), to drive the much higher resolution ocean hydrodynamic and wave models. The hydrodynamic model outputs often provide only depth-averaged two-dimensional (2D) state fields. The wave models often just provide the output of significant wave heights, wave periods, and wave directions, without

considering wave breaking processes. To overcome these deficiencies, an atmosphere-ocean-wave interactively coupled high-resolution modeling system has been developed at Coastal Carolina University and was used in conducting metocean data hindcasts. Personnel involved in this study, for the simulated atmosphere, ocean and wave components, interactively coupled several state-of-the-art public domain numerical models at CCU. The atmospheric component in the CCU coupled numerical model system is the Weather Research and Forecast (WRF; Skamarock et al., 2005) model. As a fully compressible non-hydrostatic model with a terrain-following vertical coordinate, WRF has been widely applied in applications from planetary scales down to the scales of estuarine and harbor environments. The Regional Ocean Model System (ROMS; Haidvogel et al., 2008) was employed as the ocean component. ROMS is a free-surface, hydrostatic, primitive equation model also discretized with a terrain-following vertical coordinate system. Simulations include water temperature, ocean currents, salinity, and sea surface height. ROMS can also be applied in multi-scale applications. To simulate the wind-generated ocean surface waves, which cannot be explicitly done by ROMS, a spectral wave model, Simulating Wave Nearshore (SWAN; Ris et al., 1999), was incorporated by CCU into the oceanic component. SWAN is a third-generation wave model that computes random, short-crested wind-generated surface gravity waves in coastal regions and inland water domains. Coupled with the Earth System Modeling Framework (ESMF; Hill et al., 2004), the model suite has been fully tested and thus utilized in this study.

An interactive domain grid nesting technique was implemented in the model to accommodate the integration of the atmosphere, ocean and wave components at a high resolution of 100 meters. Thus, the three nested grids with increasing spatial resolution for winds, currents, water levels and wave heights are established for the study sites. WRF provides wind forcing to ROMS and SWAN. A suite of robust physics parameterization schemes similar to those used in the operational Hurricane WRF was used in this study to represent the physical processes including microphysics, radiation, planetary boundary layer, surface layer etc. ROMS feeds back its sea surface temperature to WRF and SWAN also provides wave parameters to WRF, both of which have effects on WRF's wind simulations. Current-wave interactions between ROMS and SWAN are also represented in the model. Consideration of these interactions makes the hindcasts more realistic and are uniquely advanced over hindcast simulations which do not employ interactive numerical model coupling. The ocean hydrodynamic model ROMS is used in its full 3D capability. The oceanic wave SWAN model provides wave-breaking simulations.

The atmospheric component of the model suite, WRF, requires initial conditions, namely the 3-dimensional temperature, wind, moisture and pressure fields, at the onset of the simulation. The initial conditions were created with the NARR dataset, which covers the period 1979 to the present. Therefore, for the identified TCs that occurred prior to 1979, the dynamical WRF could not be used; instead, an empirical hurricane vortex wind model (Holland, 1981) was used to provide storm wind forcing to drive the oceanic and wave models. The empirical Holland hurricane wind model takes hurricane center pressures and location latitudes and longitudes as input, which is available in the International Best Track Archive for Climate Stewardship (IBTrACS) database, and produces outputs of cyclostrophic winds as a function of the radius distance from the storm center.

Model domain grids are configured using the bathymetry data from the U.S. Department of Commerce, National Oceanic and Atmospheric Administration, National Geophysical Data Center's 2-minute Gridded Global Relief

Data (ETOPO2v2) <http://www.ngdc.noaa.gov/mgg/fliers/06mgg01.html>. High-resolution simulations with nested grids were used.

In the ROMS model, if the bathymetry is too steep, this condition will cause computational instabilities in the ocean simulations. Therefore, by default, the ROMS model employs a smoothing algorithm to remove the steepness in bathymetry. During this case study exercise it was found that the smoothing procedures used in ROMS could cause some inaccuracies in wave simulations in shallow-water areas. A significant effort was made to revise the smoothing method so that it could remove the few steep points in the bathymetry while still retaining the accurate bathymetry in the shallow water regions for realistic simulations.

3.3. SELECTION OF STORMS FOR CASE STUDIES

To calibrate the model system, two case studies of the severe TC (Hurricane Irene in 2011) and the large ETC event (the 1993 Winter Storm) were carried out.

Hurricane Irene was a large and destructive TC that affected much of the East Coast of the United States, including several of the seven wind farm sites proposed in this study. Throughout its path, Irene caused widespread destruction and at least 56 deaths. Damage estimates throughout the U.S. have been estimated at \$15.6 billion, which made it the seventh costliest hurricane in U.S. history, behind only Hurricane Andrew of 1992, Hurricane Ivan of 2004, Hurricanes Wilma and Katrina of 2005, Hurricane Ike of 2008, and Hurricane Sandy in 2012. Its destruction and path made TC Irene a good case for a detailed hindcast and verification.

The 1993 winter storm, also known as the '93 Super storm, was a large cyclonic storm that formed over the Gulf of Mexico on March 12, 1993, and dissipated in the North Atlantic Ocean on March 15. It is unique in history for its intensity, massive size and wide-reaching effect, particularly in the southeastern U.S. and the adjacent coastal ocean zone extending across the continental margin.

These two storms were selected because: 1) both the full physics WRF model (ETC 1993 winter storm) and the empirical Holland model (TC Irene) can be examined; 2) both storms affected most of the seven selected sites; 3) there are multiple nearby buoy stations data available for model verification.

3.4. MODEL RESULTS AND VERIFICATION

TC Irene (2011)

The empirical Holland hurricane wind model was used to provide wind forcing for the ocean model ROMS and the wave model SWAN. The model outputs were compared with observation (significant wave height and 10-meter wind speed) collected from 16 nearby buoy stations (Figure 2 and Figure 3). The simulation period was from 2011-08-26-0000 to 2011-08-29-0000, with one-hour increments. All the buoy stations with valid data during the simulation period were used for the verification. Both the model outputs of the significant wave heights and 10-meter wind speeds showed very good agreement with the buoy observations, which suggests that the model suite and hindcast method was able to create a dataset that could reasonably realistically represent the

climatological met-ocean conditions at the seven proposed farm sites, and therefore, could be used to create and evaluate the hazard curves. Note NDBC Station 41048 collected wave observations during the simulation period but unfortunately its 10-meter winds were missing due to an instrument malfunction.

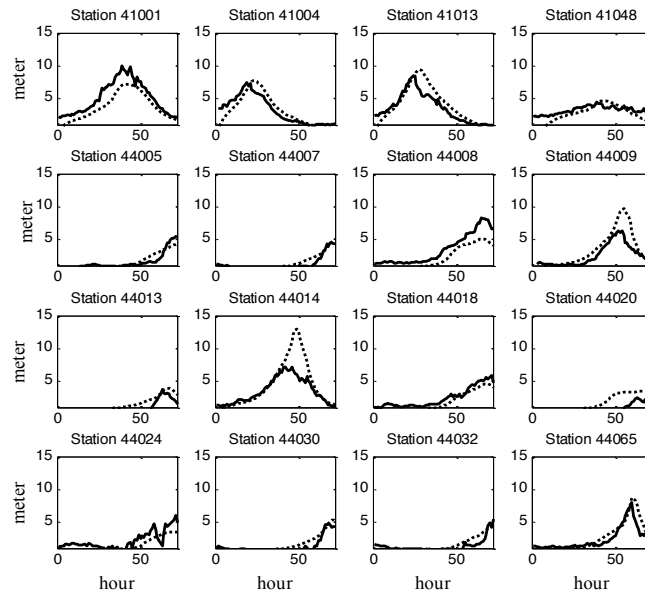


Figure 2 Comparison of significant wave heights between model output (dashed) and NDBC marine buoy station data (solid) (IRENE) (Simulation period: 2011-08-26-0000 - 2011-08-29-0000)

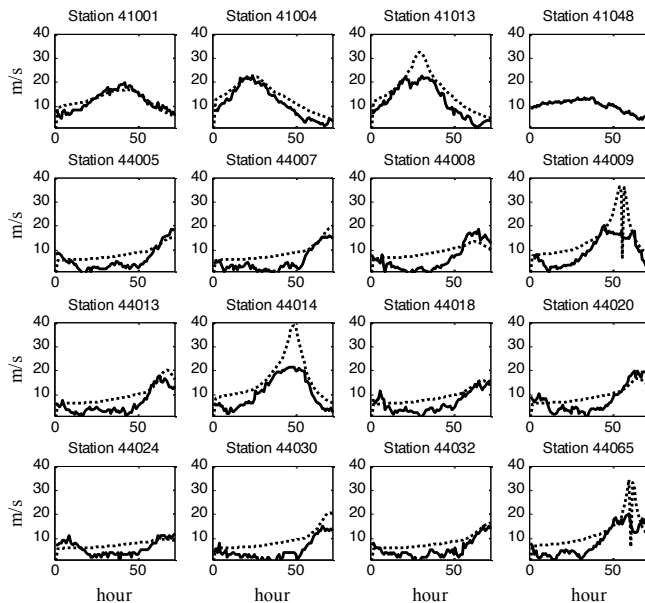


Figure 3 Comparison of 10-meter wind speed between model (dashed) and buoy station (solid) (IRENE) (Simulation period: 2011-08-26-0000 - 2011-08-29-0000)

ETC 1993 winter storm

The interactively coupled model system was used for this winter storm case simulation. The full-physics WRF model was used as the atmospheric component. All of the buoy stations with valid data during the simulation period were used for the verification. The comparison of model and observation are shown in Figure 4 and Figure 5. The simulation period was two days from 1993-03-13-06:00 to 1993-03-15-06:00. Note NDBC Station 44005 recorded significant wave height data, but its 10-meter wind data was missing due to an instrument malfunction. Model output showed reasonably good agreement with observations for both 10-meter winds and significant wave heights, which suggests that the model suite and hindcast method was able to create a dataset that could reasonably realistically represent the climatological met-ocean conditions at the seven proposed farm sites, and therefore, could be utilized in the creation and evaluation of the hazard curves.

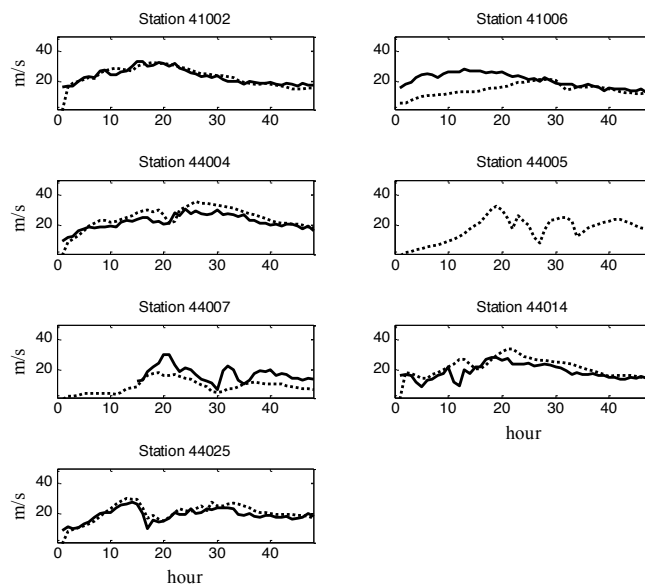


Figure 4 Comparison of wind speed between model (dashed) and buoy station (solid) (1993 Winter Storm) (Simulation period: 1993-03-13-0600 - 1993-03-15-0060)

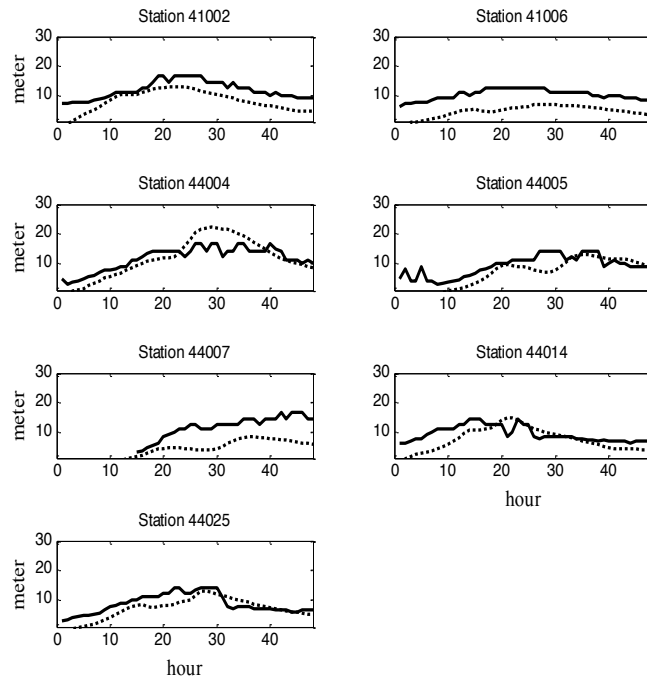


Figure 5 Comparison of significant wave height between model (dashed) and buoy station (solid) (1993 Winter Storm) (Simulation period: 1993-03-13-0600 - 1993-03-15-0060)

4. Storm Hind-cast and Development of Metocean Hazard Curves

With approval from BSEE, we conducted the production hind-cast modeling of the TC and ETC storms affecting the 7 selected sites as initially proposed. High performance computation (HPC) facilities at Coastal Carolina University and the Texas Advanced Computing Center sponsored by the Extreme Science and Engineering Discovery Environment (XSEDE) program. All of the identified TC and ETC storms have been hind-cast using the methods described above.

The “Generalized Extreme Value Distribution” method was used in developing the exceedance curves. The method is described at <http://www.mathworks.com/help/stats/generalized-extreme-value-distribution.html>

At first the 10-meter wind and significant wave height modeling results at the locations listed in Table 1 and labeled by the yellow marks in Figure 1 were extracted and the exceedance curves were constructed. However, it was found that some of the site locations in Table 1 have a water depth that is shallow enough so that its wind-induced surface wave height is limited by the shallow bathymetry due to wave breaking processes. This is illustrated in Figure 6. The significant wave height curve for site 3 had a flat shape at the high-value end, whereas the curve for wind had a non-zero slope. This indicated that even when the surface wind strength increased at the high-value end of the wind curve, the significant wave height curve did not respond to the increased wind strength and remained flat, due to the wave breaking process.

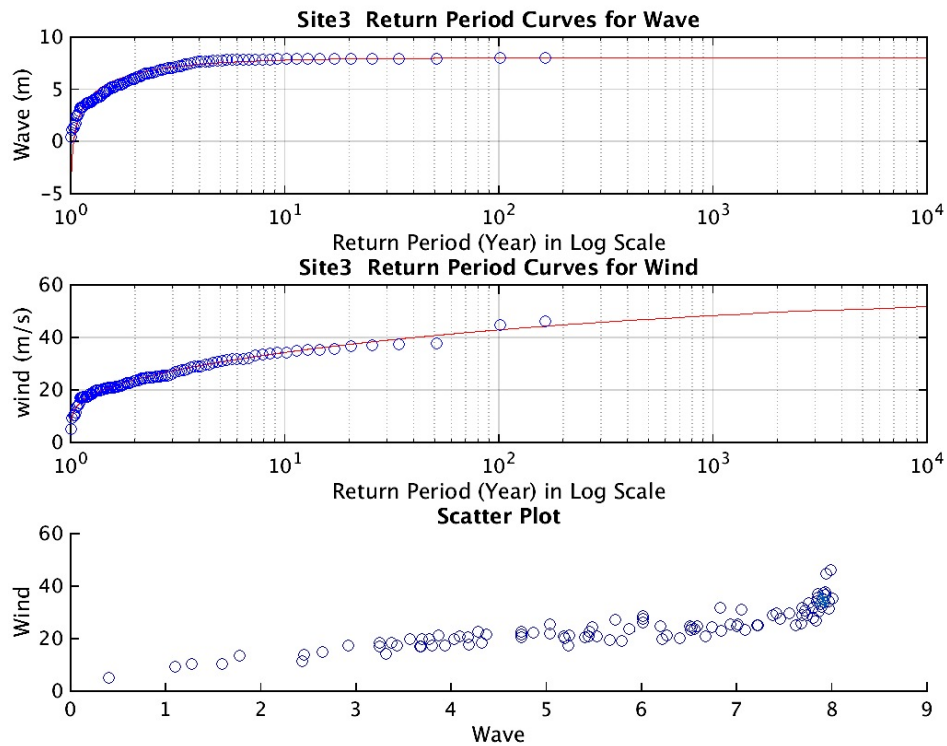


Figure 6 Site 3 exceedance curves of wave height (upper panel) and wind strength (middle panel), and the wind-wave scatter plot (bottom panel), at site 3's original location with shallow water

The flat exceedance curves of significant wave height at the shallow locations are shown in Figure 6. However, we noted that a realistic depiction of the wave breaking process posed a difficulty for further load factor analyses at these sites. Therefore, we changed the data extraction locations slightly to the ones marked by cyan place markers in Figure 1 so that the water depths at the new locations are deep enough so that they do not limit the significant wave height values (Figure 7). Figure 8 shows the exceedance curves for surface wind strength and significant wave height at all the 7 selected wind farm sites, at their revised locations with deep water depths.

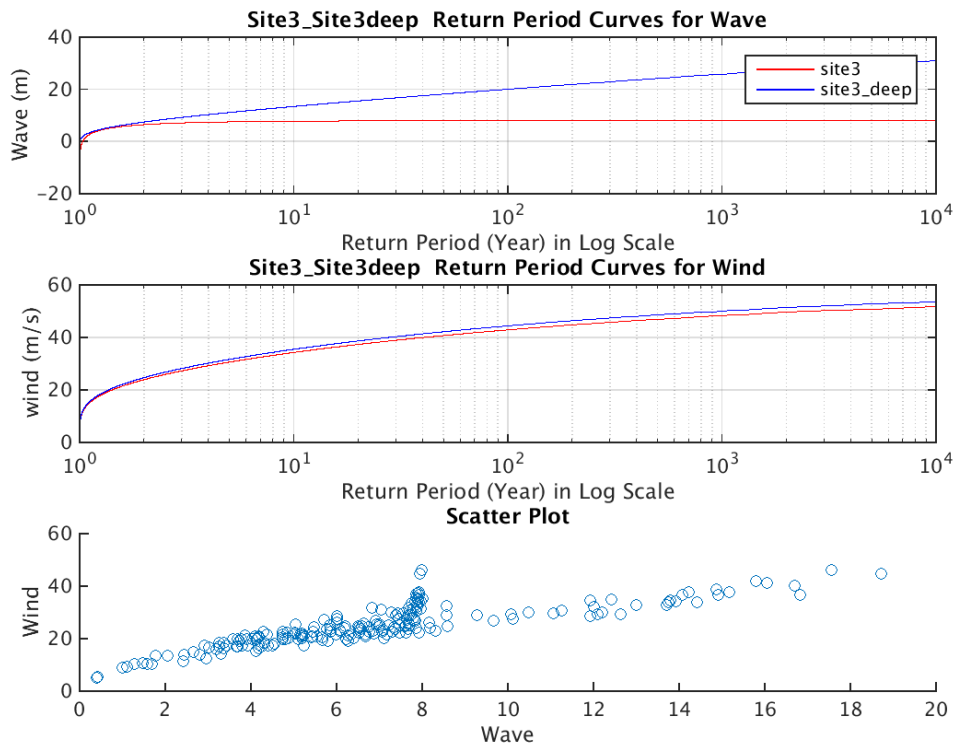


Figure 7 Site 3 exceedance curves of wave height (upper panel) and wind strength (middle panel), and the wind-wave scatter plot (bottom panel), at site 3's revised location with deep water. Note the scatter plot contained both shallow and deep water model data at site 3.

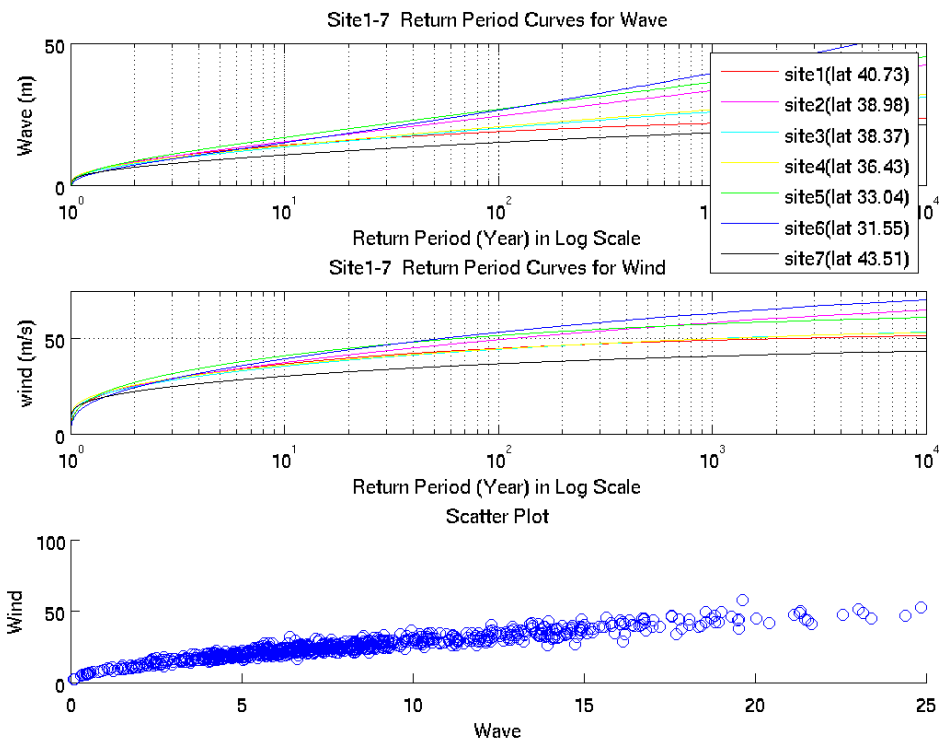


Figure 8 The exceedance curves of wave height (upper panel) and wind strength (middle panel), and the wind-wave scatter plot (bottom panel) for all the selected wind farm sites, at their *revised* location with *deep* water.

For ETC storms, the wave and wind exceedance curves were made from model hind-casts of storms that happened between 1979 and 2014, as proposed in the project proposal. ETC storms usually cause surface wind strengths and significant wave heights that are far weaker than those caused by TC storms. Therefore, due to the relatively short ETC data coverage (compared to the TC storms database that ranged from 1851 to 2013), ETC curve shapes may be sensitive to a small number of extraordinarily strong wind and wave events. It was found that the 1993 winter storm is an example of such an extraordinarily strong event. The 1993 winter storm, which had the wind strength equivalent to a Category-2 hurricane, caused extraordinary high waves over most of the seven selected regions due to its strong wind, very large impact area, large fetch, and long acting time. The high waves caused by this 1993 winter storm far exceeded those caused by other ETCs (as shown in the plots of NOAA marine buoy data in Pietrafesa et al., 2015). This single event dominated the wave height ETC exceedance curve due to the relatively short 35-year data base or ETC, which caused difficulties for the MMI team members to use the ETC exceedance curves to analyze load factors in the subsequent tasks. Figure 9 and Figure 10 show that if the 1993 super storm had been excluded, the curves (in red) would have a more “expected” linear or concave shape. However, with the 1993 ETC included in the analysis results, the site 1 and site 5 curves (in blue) showed a convex shape, which is considered abnormal and posed difficulty for further load factor analyses.

This issue was caused by the extraordinarily strong 1993 ETC event in a relatively short 35-year ETC data length. We evaluated alternative algorithms to better represent a single extreme event in a relatively short database in the exceedance curves. We have also proposed to double the ETC data length by including a supplement, lower resolution database, that dates back to 1950, hopefully to capture some strong events to fill the gap between the typical ETC storms and the “storm of the century” in 1993. In consultation with BSEE staff, the determination was made to include the additional database to extend the time series to address clear biasing to the exceedance curves and associated effects on potential load factor calculations and to focus on these primary objective of the project of providing comparison of load factors across the various wind energy areas along the east coast, of the US.

The additional model hind cast using the supplemental database and its results are described below.

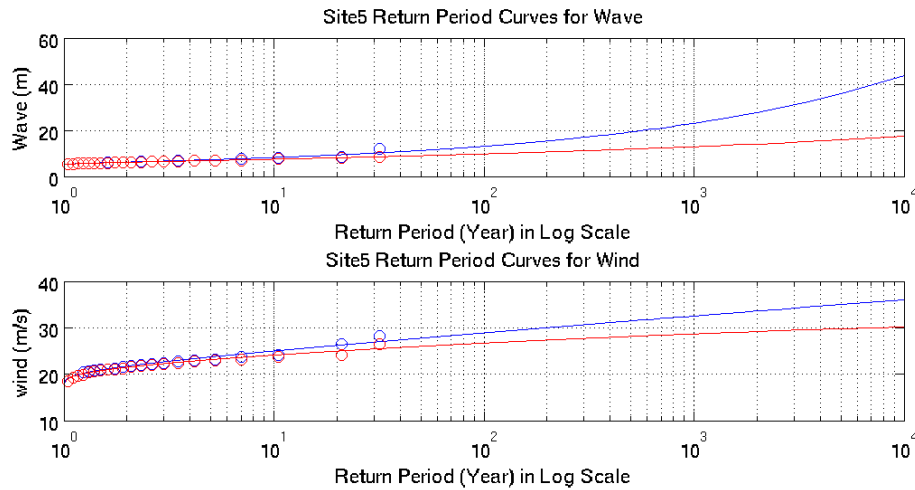


Figure 9 Exceedance curves of *ETC* significant wave height (upper panel), 10-meter wind (bottom panel) for site 5 with (blue curves) and without (red) the 1993 ETC data.

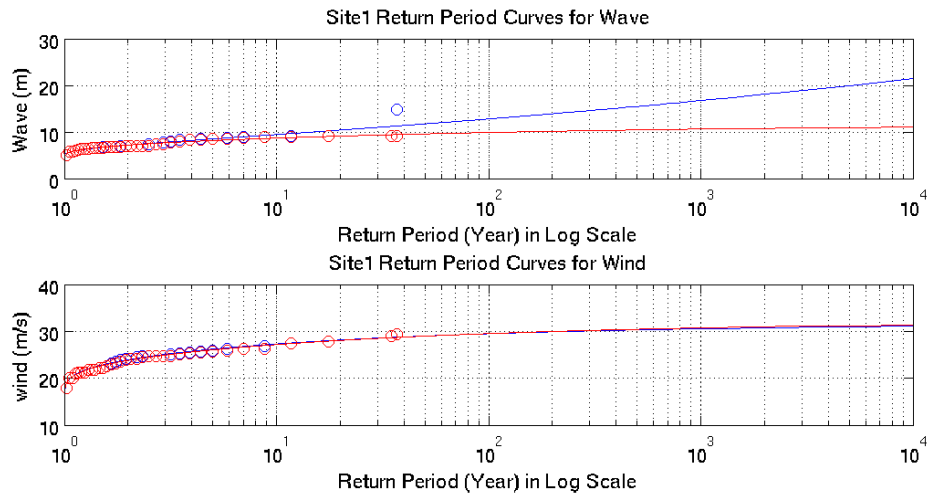


Figure 10 Exceedance curves of *ETC* significant wave height (upper panel), 10-meter wind (bottom panel) for site 1 with (blue curves) and without (red) the 1993 ETC data.

5. Supplemental Extra-Tropical Storm Database

Preliminary evaluation of the exceedance curves showed that for some of the sites, very strong winter storms, such as the “storm of the century” nor’easter in 1993, caused dramatic impacts on the shape of the surface wave hazard curves. Following discussion with BSEE staff, we resolved this issue by including a supplemental database to increase the sample size of ETCs. The increased sample size allowed the extraordinary 1993 winter storm to have a longer return period, which made the hazard curves to have a smoother slope into the higher return periods.

The supplemental database we used is an atmospheric reanalysis developed by the NOAA’s National Centers for Environmental Prediction (NCEP) and the National Center for Atmospheric Research (NCAR). The NCEP/NCAR database includes the reanalysis of atmospheric state variables that spanned from 1948 to 1978. The wind speed at 10-m altitude was used in this task to identify storms for the selected seven sites. The algorithm for identifying storms for the selected seven sites is the same as the method used for previous tasks. A total of ~ 800 ETC events were identified for the seven selected sites. All the identified ETC events were simulated using the coupled WRF-ROMS-SWAN model with the initial and lateral boundary conditions downscaled from the NCEP/NCAR reanalysis dataset. The simulated 10-m winds and surface waves were then extracted and post-processed to construct the hazard curves.

5.1. CURVES FOR ETC+TC CASES

Figure 11 and Figure 12 show the curves for both the total ETC+TC storm cases when the combined original and supplemental dataset (Figure 11) or the original dataset only (Figure 12) is used. The inclusion of the supplemental dataset did not change the total time span of dataset because the period of the supplemental dataset, 1948-1978, is already included in the original ETC+TC dataset, which is 1851-2013. Therefore, the inclusion of the supplemental dataset did not cause significant changes in the shapes of the curves for ETC+TC.

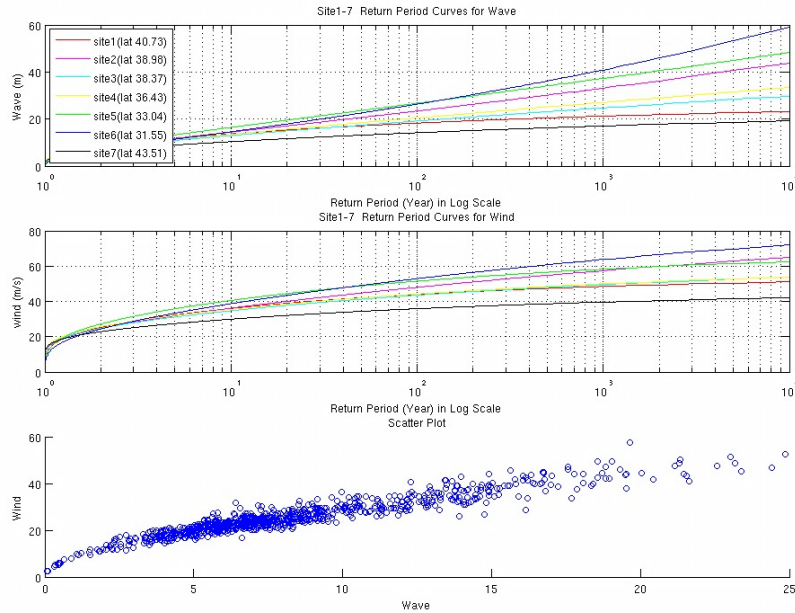


Figure 11 Wave (upper panel) and wind (middle panel) hazard curves for the seven selected sites. The bottom panel shows the scatter plot of the simulated maximum winds vs. maximum waves. The *original and supplemental* data sets are included. The curves are for both *TC and ETC* storm cases.

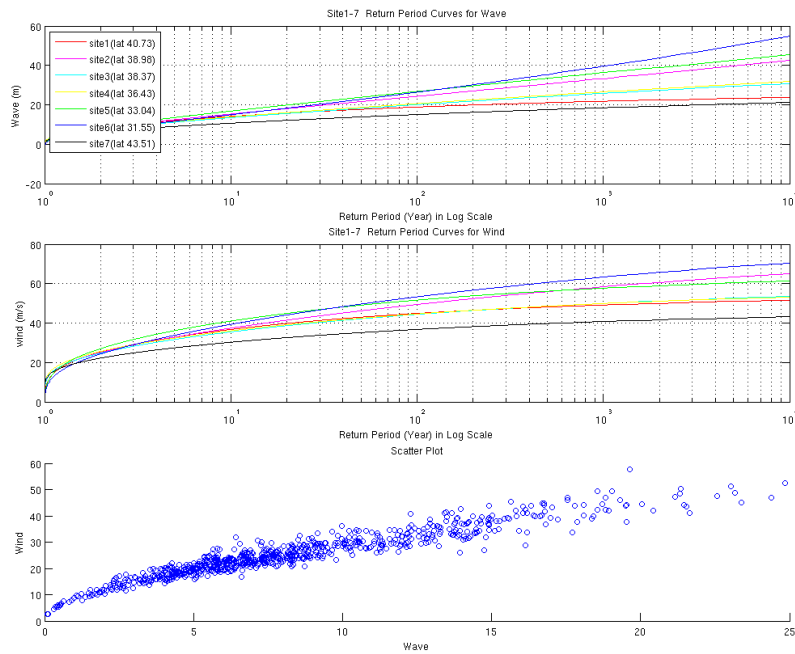


Figure 12 Wave (upper panel) and wind (middle panel) hazard curves for the seven selected sites. The bottom panel

shows the scatter plot of the simulated maximum winds vs. maximum waves. Only the *original* data set is included. The curves are for both *TC and ETC* storm cases.

5.2. CURVES FOR ETC-ONLY CASES

Figure 13 and Figure 14 show the curves for the ETC cases only when the combined original and supplemental dataset (Figure 13) or the original dataset only (Figure 14) were used.

The inclusion of the supplemental dataset did change the total time span of ETC dataset because the period of the supplemental dataset, 1948-1978, was not included in the original ETC+TC dataset, which is 1979-2013.

The inclusion of the supplemental dataset did cause significant changes in the shapes of the hazard curves for the surface wave. Most noticeably, for the site-5 and site-6, the steep slopes of the surface wave hazard curves using only the original dataset (green and blue curves in the upper panel of Figure 14) were eliminated when the supplemental dataset was included (upper panel of Figure 13). The differences between Figure 13 and Figure 14 are most evident for site-5 and site-6, probably because the original ETC datasets for these two sites had relatively small sample sizes. Therefore, the inclusion of the supplemental datasets significantly increased the total ETC sample sizes for the site-5 and site-6, thus significantly changed their curve shapes.

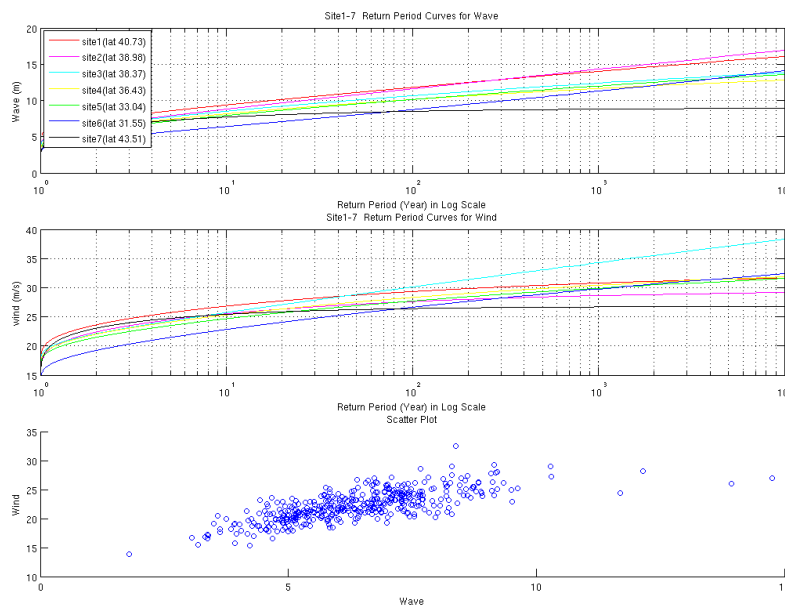


Figure 13 Wave (upper panel) and wind (middle panel) hazard curves for the seven selected sites. The bottom panel shows the scatter plot of the simulated maximum winds vs. maximum waves. Both the *original and supplemental* data sets are included. The curves are for *ETC only* storm cases.

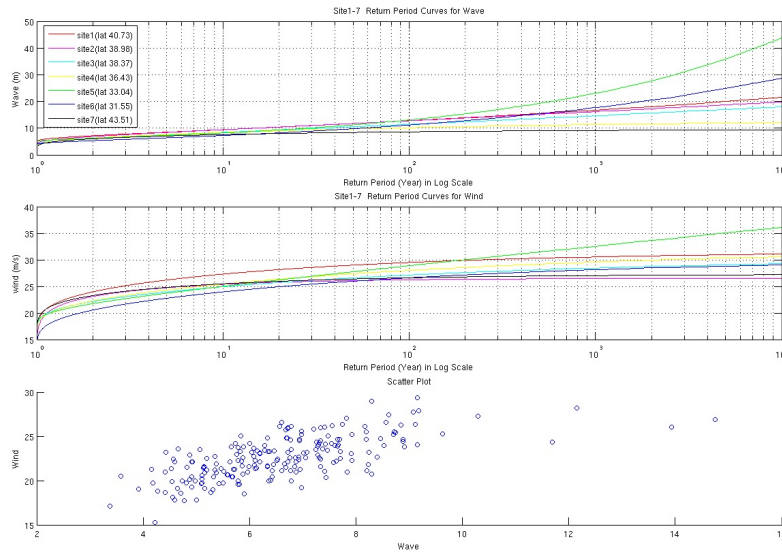


Figure 14 Wave (upper panel) and wind (middle panel) hazard curves for the seven selected sites. The bottom panel shows the scatter plot of the simulated maximum winds vs. maximum waves. The *original* data set is included. The curves are for *ETC only* storm cases.

Values of the newly created hazard curves using the combined original and supplemental datasets, for the ETC-only and the total ETC+TC cases, respectively, have been used by MMI Engineering for load factor analysis.

6. Load Factor Calibration Study

The objective of this study was to determine the adjustments to load safety factors that are needed to achieve system reliability indices that are uniform across regions without tropical storm hazards (i.e., the generic IEC application) and those for which met ocean exceedance data has been generated. These load factors could be derived using an absolute analysis in which failure probabilities or reliability indices could be calculated for specific site conditions, turbine types, etc. However, such an approach would require the definition of a maximum permissible failure probability, which is not readily available, and an extensive number of analysis cases. Instead, a relative analysis approach was adopted where the target performance objective was defined based the IEC load factors for East Coast metocean conditions that exclude tropical storms. The addition of tropical storms to the metocean conditions then determined the extent of load increase from the design levels and the associated increase in load factor that is needed to produce similar levels of performance across all the selected areas.

The structural demand was defined on the basis of load which is determined through analysis using the wave heights and wind speeds defined in the earlier tasks. At this stage, it was not possible to perform an explicit analysis of multiple structure types in varying water depths and site conditions; therefore, a single design parameter, the demand from 50-year ETC multiplied by a load factor of 1.35, was used as the basis of comparison. As the majority of the support structures used for offshore wind turbines are more sensitive to mudline overturning moment (OTM) than they are to mudline base shear, mudline overturning moment was used as the measure of the storm demand in this study. The overturning moment exceedance curves were developed using the wind and wave exceedance curves developed both for ETCs and TCs in the previous tasks. As the slope of the ETC exceedance curves varies between sites, the return period of the target demand varies from site to site. The comparison between the return periods of the target demands illustrates the variation in the reliability indices achieved despite the fact that the same IEC load factor of 1.35 was applied at all the sites.

The generated OTM exceedance curves were also used to define a load factor for TCs to be able to achieve the same target return period (and hence, the same reliability index) as the IEC design approach. The new load factors were obtained by taking the ratio of the OTM demand by the TCs with target return period and 50-year return period. The second comparison between the sites was made using these load factors.

The results of the load factor calibration study are provided below.

6.1. WIND AND WAVE EXCEEDANCE CURVES

The wave and wind exceedance curves provided by CCU for all the 7 selected sites are shown below in Figure 15-21. Each plot contains two curves: (1) the exceedance curve developed only using extra-tropical cyclone (ETC) database and (2) the exceedance curve developed using both extra-tropical and tropical cyclone (ETC+TC) databases.

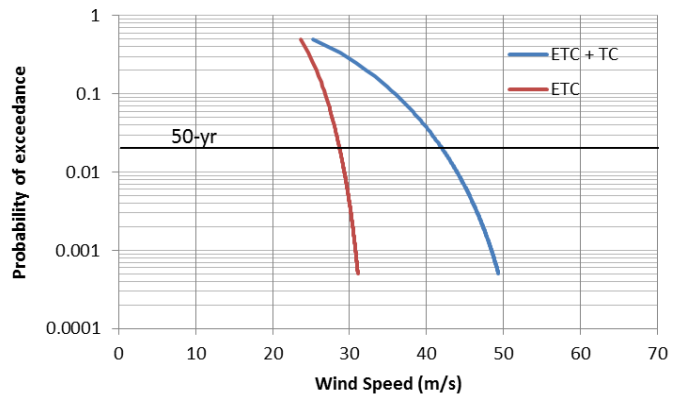
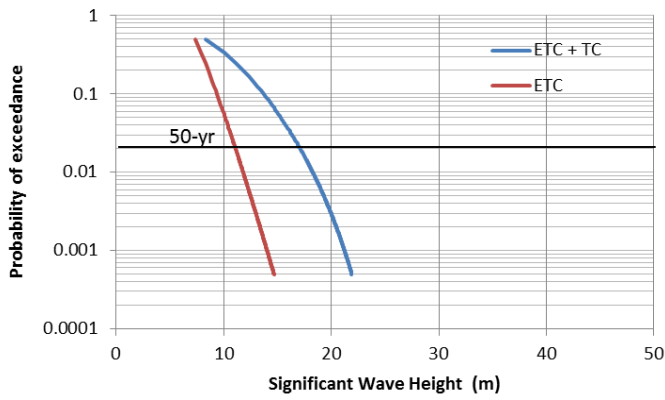


Figure 15 Wave and Wind Exceedance Curves for Site 1

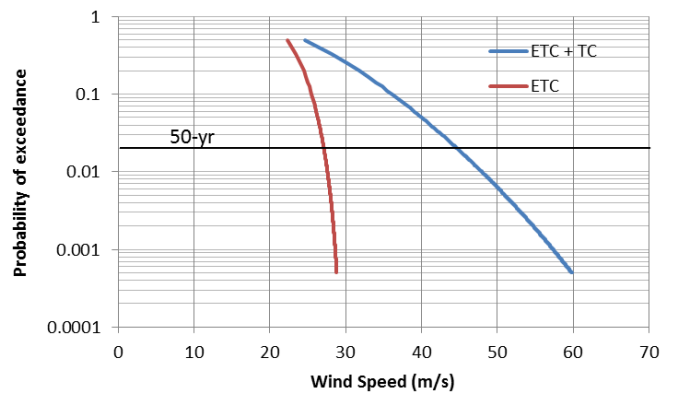
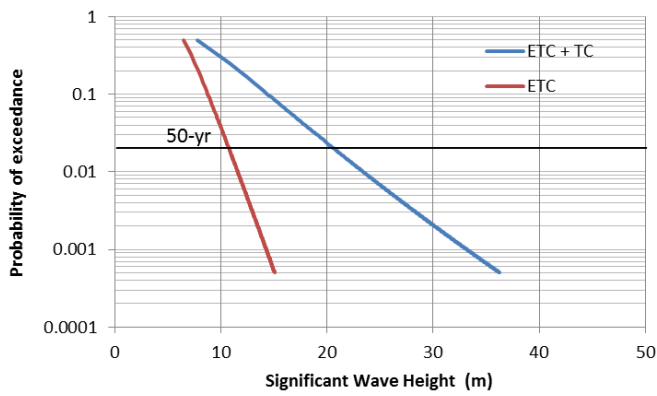


Figure 16 Wave and Wind Exceedance Curves for Site 2

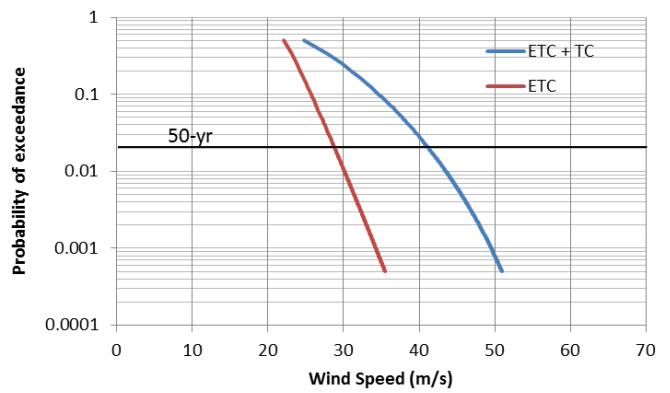
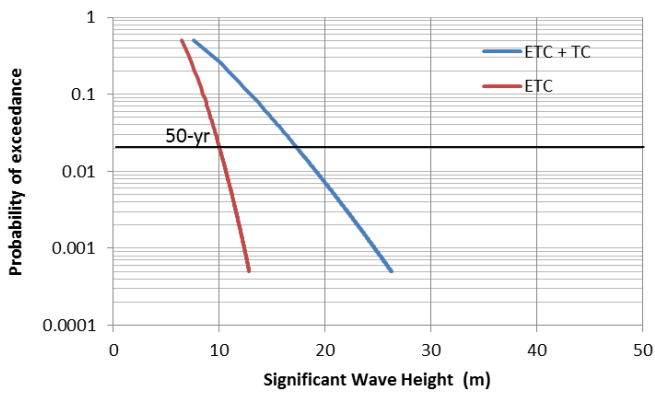


Figure 17 Wave and Wind Exceedance Curves for Site 3

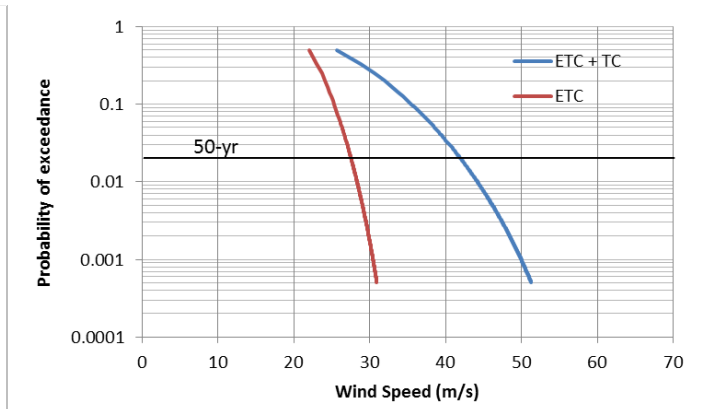
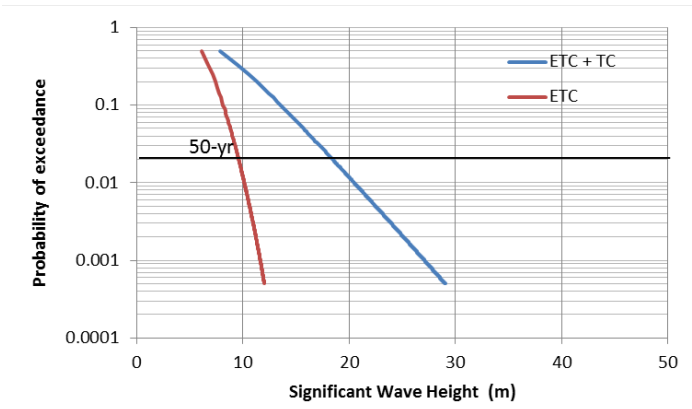


Figure 18 Wave and Wind Exceedance Curves for Site 4

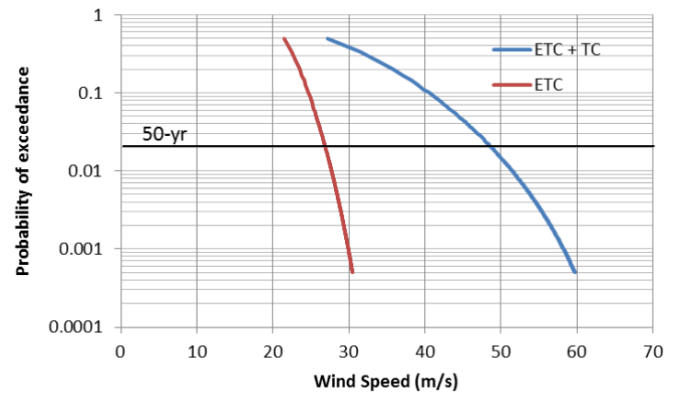
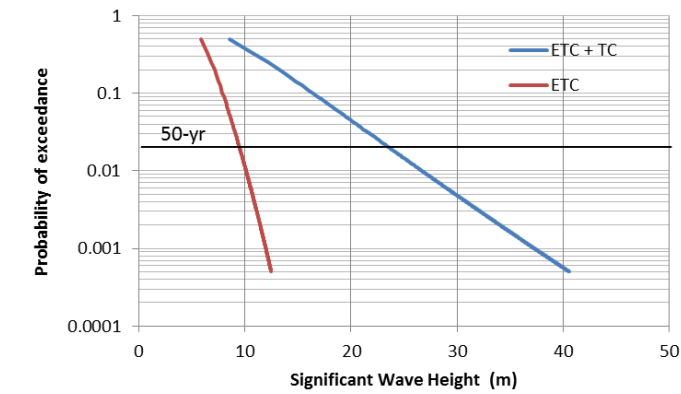


Figure 19 Wave and Wind Exceedance Curves for Site 5

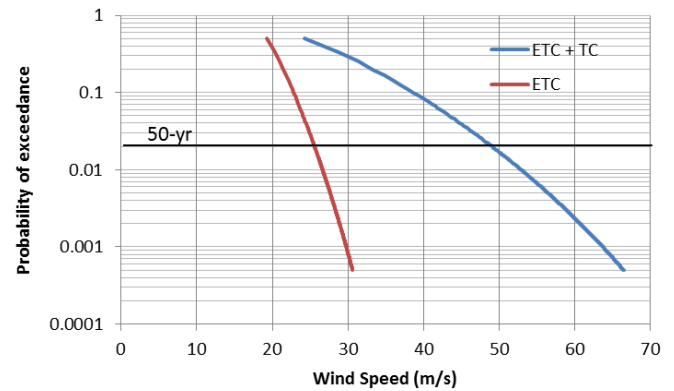
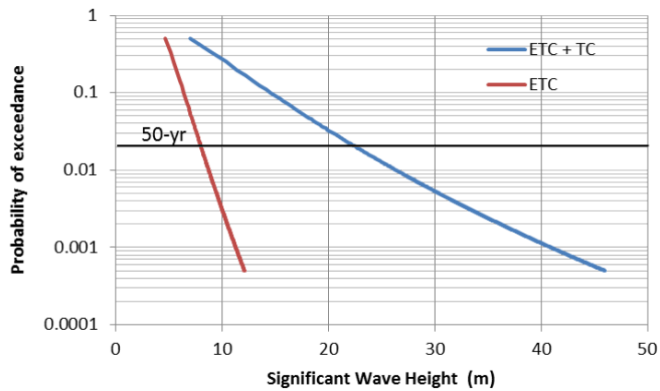


Figure 20 Wave and Wind Exceedance Curves for Site 6

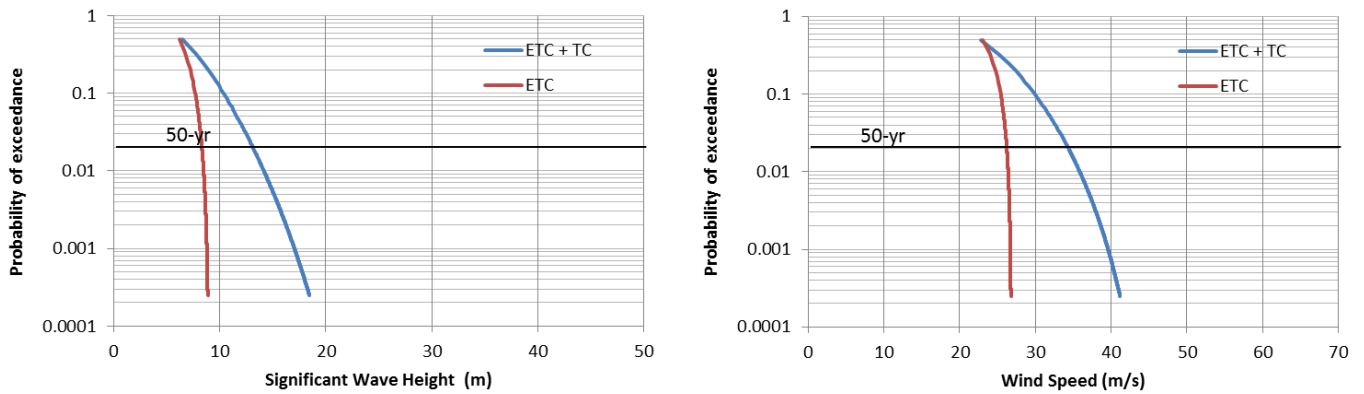


Figure 21 Wave and Wind Exceedance Curves for Site 7

6.2. APPROACH

The load factors could be calibrated using an absolute analysis in which failure probabilities or reliability indices could be calculated for specific site conditions, turbine types, etc. However, such an approach would require the definition of a maximum permissible failure probability, which is not readily available, and an extensive number of analysis cases. Instead, a relative analysis approach was adopted for this study. The target performance objective was defined based on IEC load factors for East Coast metocean conditions that exclude tropical storms. The addition of tropical storms to the metocean conditions would then determine the extent of load increase from the design levels and the associated increase in load factor that is needed to produce similar levels of performance across all the selected areas.

The structural demand is characterized on the basis of load which is determined through analysis using the wave heights and wind speeds defined previously. At this stage, it was not possible to perform explicit analysis of multiple structure types in varying water depths and site conditions; therefore, a single design parameter was selected as the demand from a 50-year ETC multiplied by a load factor of 1.35. Overturning moment (OTM) at the mudline was used as the measure of the storm demand in this study. Overturning moment exceedance curves were developed using the wind and wave exceedance curves developed both for ETCs and TCs in the previous tasks. As the slope of the ETC exceedance curves varies between sites, the return period of the target demand varies from site to site. The comparison between the return periods of the target demands illustrates the variation in the reliability indices achieved despite the fact that the same IEC load factor of 1.35 was applied at all the sites.

The generated OTM exceedance curves were also used to define a load factor for TCs to be able to achieve the same target return period (and hence, the same reliability index) as the IEC design approach. The new load factors were obtained by taking the ratio of the OTM demand by the TCs with target return period and 50-year return period. The second comparison between the sites was made using these load factors.

For a storm with a given return period, the OTM at the mudline are considering the following:

- The OTM demand from an X-year storm was estimated assuming X-year wind and X-year wave criteria occurring concurrently.
- Coupling of wind and wave forces was excluded.

- Slam load from a breaking wave condition was excluded.
- The uncertainties on the resistance side were assumed to be uniform across all sites.

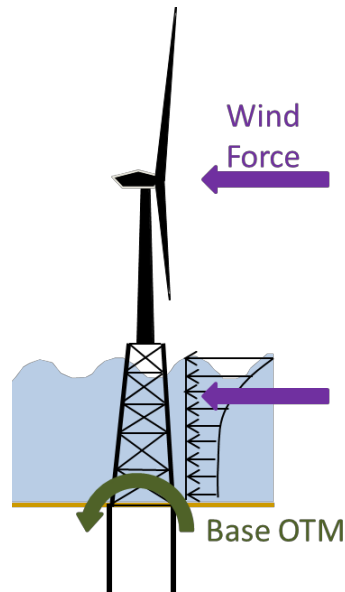


Figure 22 Storm Effects on a Wind Turbine

The wind load calculations are based on NREL 5MW reference turbine. The hub height of this turbine is at 89.5 m elevation from the water surface. A transfer function was developed using the results of the coupled analyses during the JIP performed by MMI. The wind transfer function is shown below. For the given wind speed range, the turbine remains shut down (i.e. the blades are parallel to the wind)

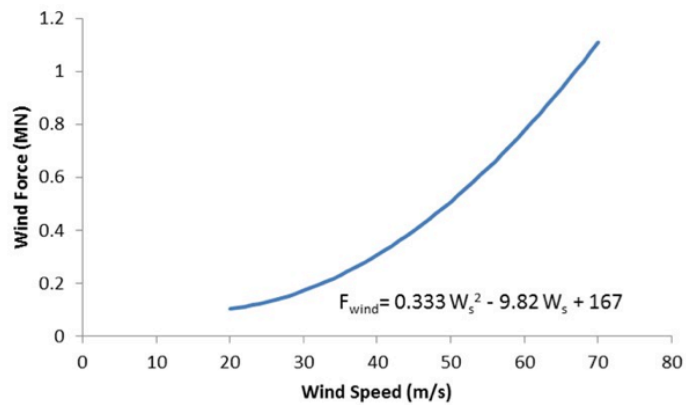


Figure 23 Wind Transfer Function

Similarly, a transfer function was also developed for the wave loading. The transfer function is based on a

generic site with 50m water depth. For any given significant wave height (H_s), water particle kinematics was calculated using the corresponding H_{max} and T_{max} :

$$H_{max} = 2.14 (H_s^{0.872})$$

$$T_z = 4.29 (H_s^{0.351})$$

$$T_{max} = 1.2 * T_z$$

Sum of the width of all structural members were assumed as uniform along the height. Wave force was calculated at the crest location using Morisson Equation. The wave transfer function is shown below. The centroid of the wave force is approximately at $0.73(\text{Water Depth} + 0.6H_s)$.

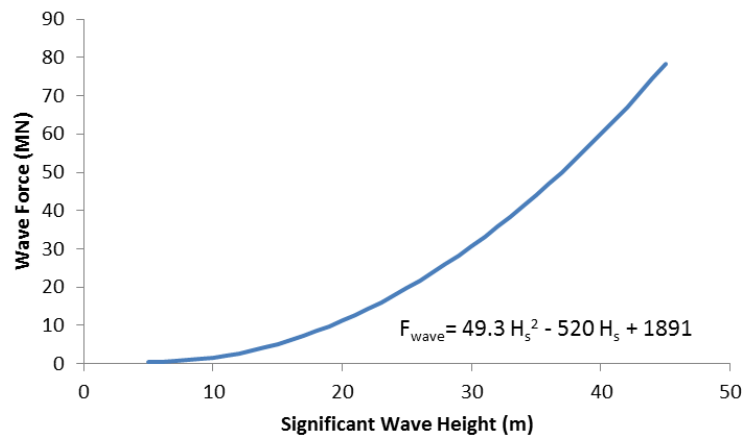


Figure 24 Wave Transfer Function

6.3. MUDLINE OTM EXCEEDANCE CURVES

The wind and wave transfer functions above were used to develop mudline OTM exceedance curves provided below.

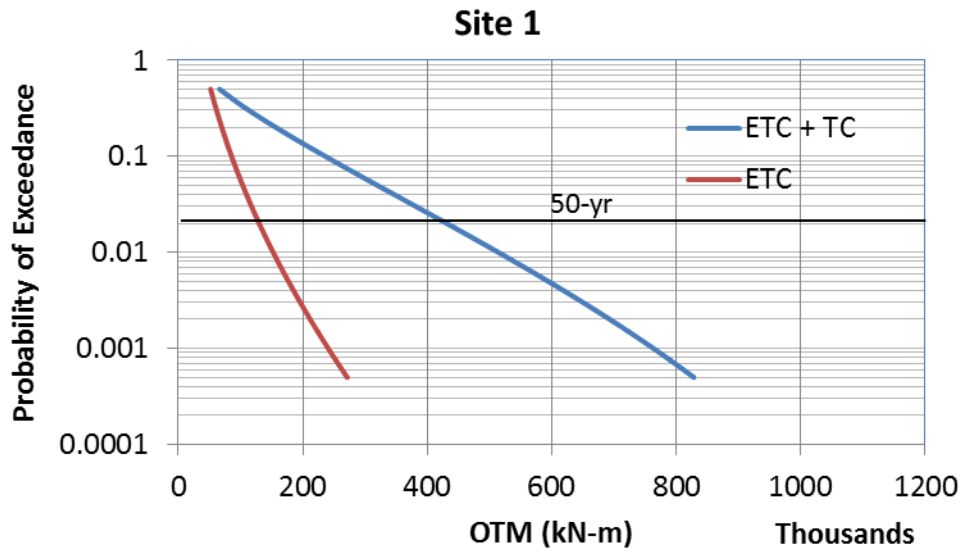


Figure 25 Base OTM Exceedance Curve for Site 1

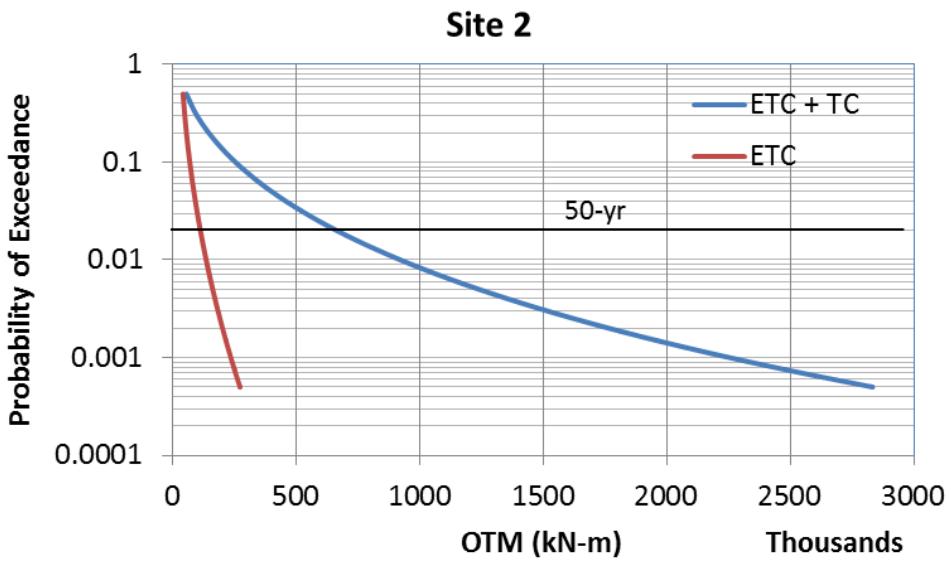


Figure 26 Base OTM Exceedance Curve for Site 2

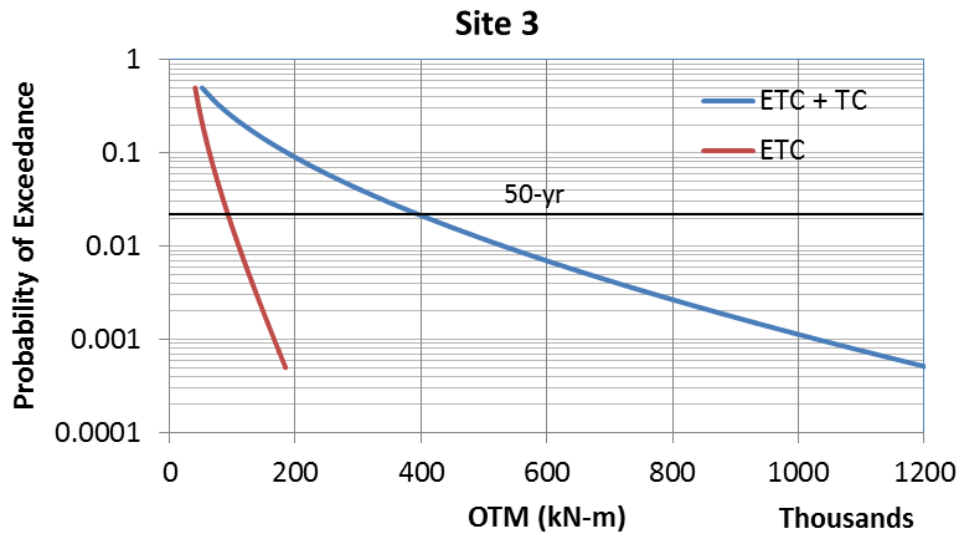


Figure 27 Base OTM Exceedance Curve for Site 3

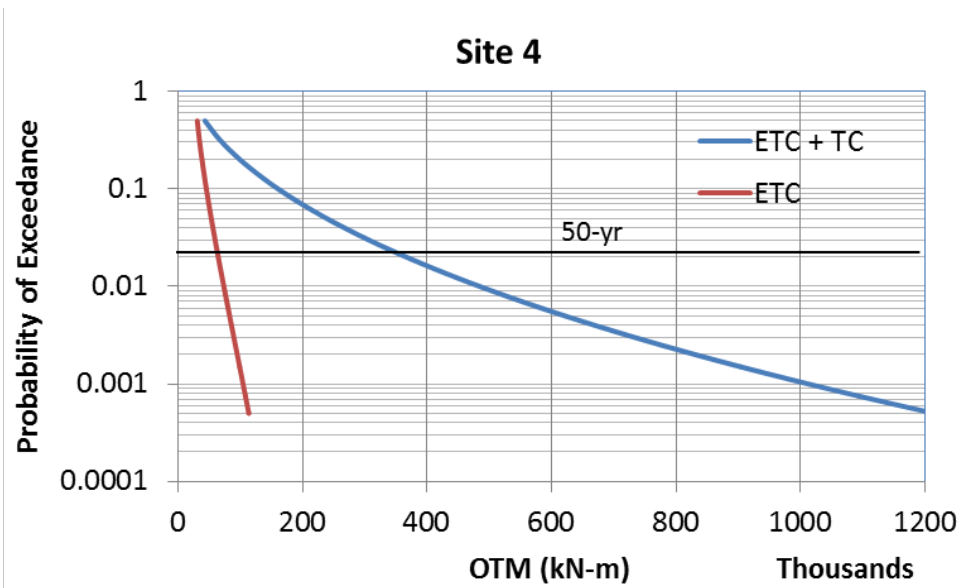


Figure 28 Base OTM Exceedance Curve for Site 4

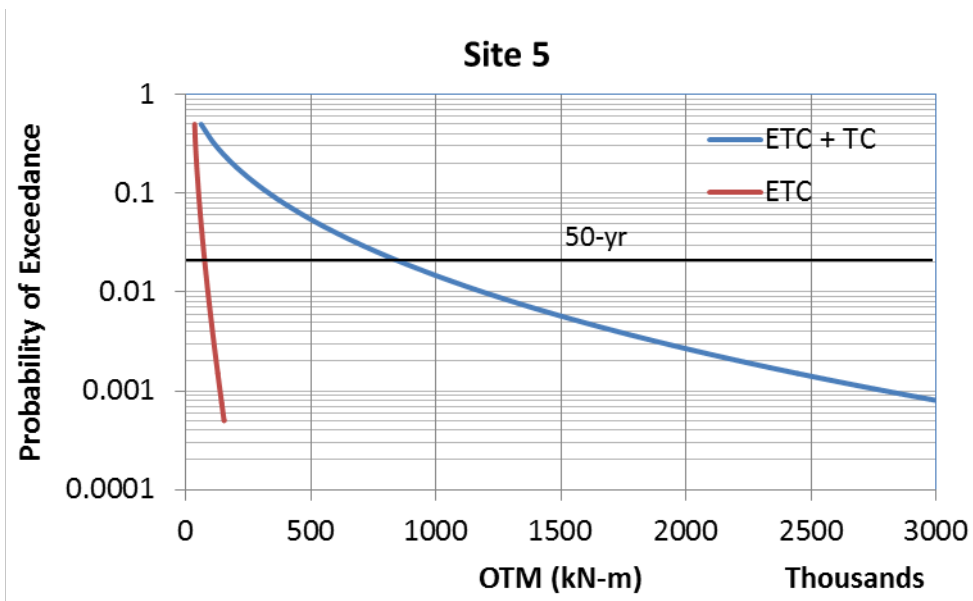


Figure 29 Base OTM Exceedance Curve for Site 5

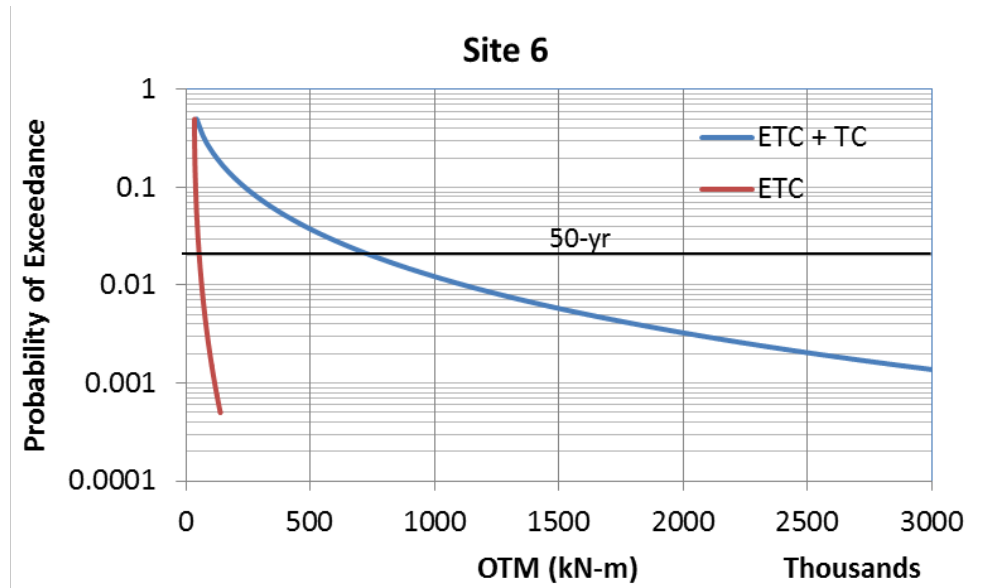


Figure 30 Base OTM Exceedance Curve for Site 6

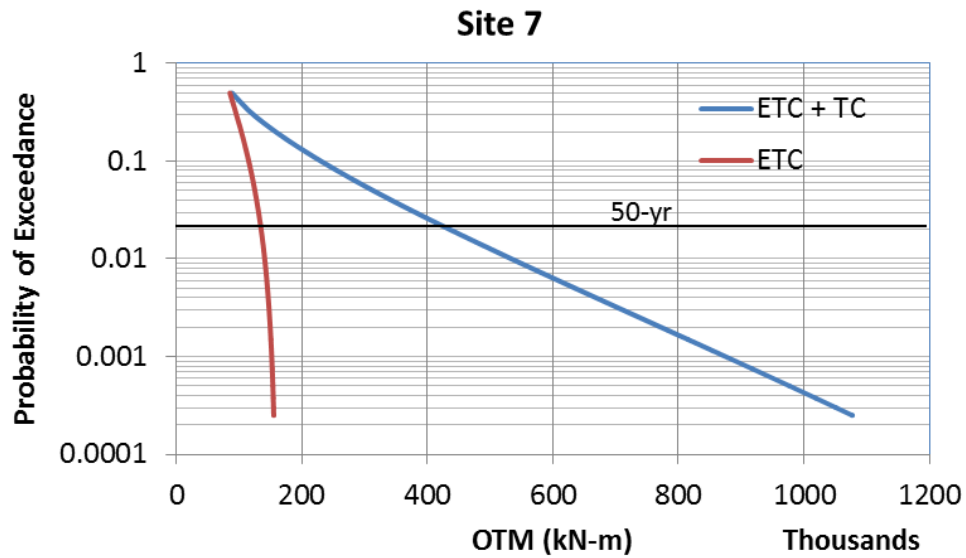


Figure 31 Base OTM Exceedance Curve for Site 7

6.4. CALCULATION OF LOAD FACTORS FOR TROPICAL CYCLONES

The load factors for TCs were estimated using the mudline OTM exceedance curves. The procedure is illustrated in Figure 32. The procedure is as follows:

- On the red ETC curve, the mudline OTM for a 50-year storm (probability of exceedance of 0.02) is 112×10^3 kN-m.
- The target design demand is equal to $1.35 \times 112 \times 10^3$ kN-m = 152×10^3 kN-m.
- The probability of failure for 152×10^3 kN-m is 0.00654 which is equivalent to a return period of 153 years.
- The 50-year and 153-year return period mudline OTMs from the ETC+TC curve are 664×10^3 kN-m and $1,110 \times 10^3$ kN-m, respectively.
- The load factor for ETC+TC is calculated is $1,110 \times 10^3$ kN-m / 664×10^3 kN-m = 1.67.

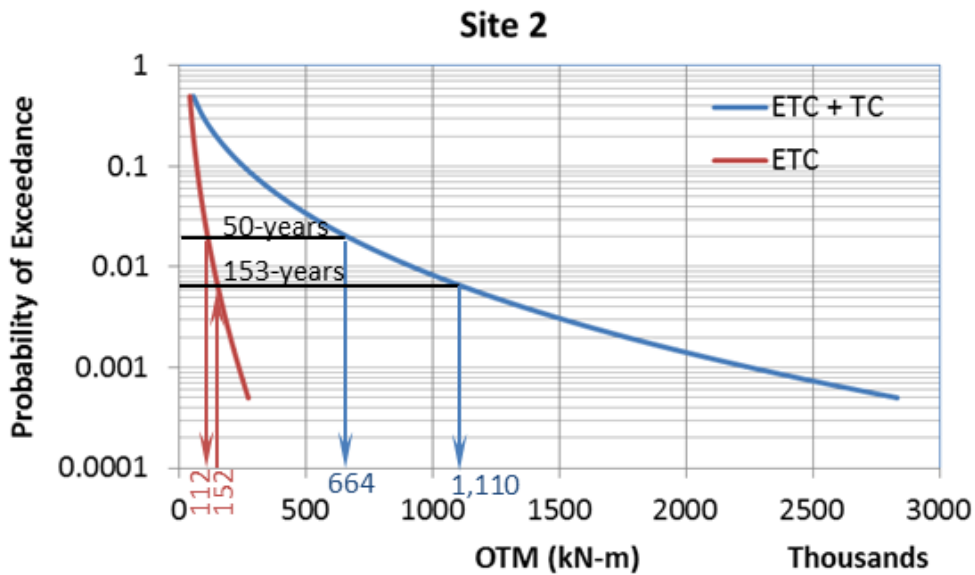


Figure 32 A Sample Case for Load Factor Estimation for TCs

Table 2 lists the estimated load factors for the selected sites. Key observations in the provided results are as follows:

- For Sites 1 through 6, the target return period obtained using the standard IEC load factor of 1.35 ranges between 153 years to 276 years.
- For Sites 1 through 6, the load factor estimates for TCs range between 1.37 (in the north where TCs are weaker) and 1.94 (in the south where the TCs are stronger).
- For Site 7, 1.35 times the 50-year mudline OTM exceeds the range of the developed wind and wave exceedance curves (i.e. 4,000 years). Note that the ETC wind and wave exceedance curves in Figure 21 remain constant as the failure probability decreases (or the return period increases). A similar tendency is also reflected on the mudline OTM exceedance curve for ETC in Figure 31.

Table 2 Comparison of Load Factors for Selected Sites

Site			Extra Tropical Cyclones(ETC)			Including Tropical Cyclones (ETC+TC)		
No	Location	Water Depth (m)	50-year OTM (MN-m)	1.35 x 50-year OTM (MN-m)	Equivalent Return Period (years)	50-year OTM (MN-m)	OTM for Target Return Period (MN-m)	Load Factor
1	Massachusetts and Rhode Island	60	130	175	192	431	590	1.37
2	New Jersey	56	112	152	153	664	1,110	1.67
3	Maryland	54	94.8	128	213	411	680	1.65
4	Virginia and North Carolina	38	64.6	87.3	276	367	691	1.88
5	Longbay	50	76.3	104	204	864	1,595	1.84
6	Savannah	48	52.3	70.6	162	750	1,451	1.94
7	Maine	140	135	183	2000+ (Exceeded chart limit)	436	N/A	N/A

To be able to make a graphical comparison between the base OTM exceedance curves for ETC and ETC+TC, the curves were normalized with respect to their value at 50-year return period (or probability of exceedance of 0.02). The normalized base OTM exceedance plots are provided below. The horizontal axis in the plots shows the normalized OTM which is also equivalent to load factors.

The normalized plot for Site 1 shows that the slope of the ETC and ETC+TC exceedance curves are almost identical for return periods over 50 years (or probability of failure less than 0.02). As a result of this, there is almost no adjustment needed due to tropical cyclones at this site.

On the other hand, the slopes of the two normalized curves for Site 6 are quite different. Therefore, Site 6 will require a much higher load factor due to tropical cyclones.

The problem associated with the load factor calculation for Site 7 also becomes visible when the curves are normalized. As seen in the plot, the red exceedance curve for ETC does not exceed 1.35 in the horizontal axis. This is because the shape of the curve (i.e. concave) is also rather different than all the other normalized exceedance curves (ETC or ETC+TC) which are either convex or close to linear.

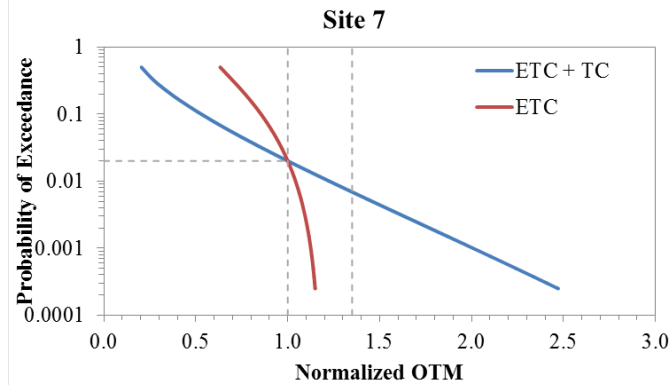
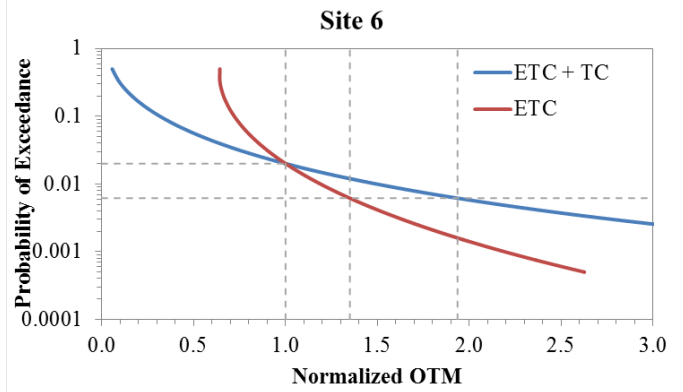
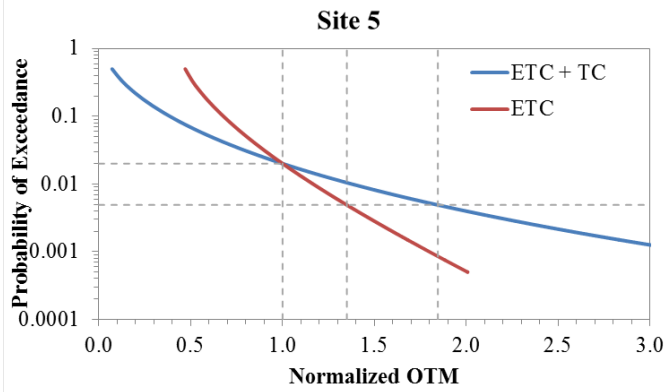
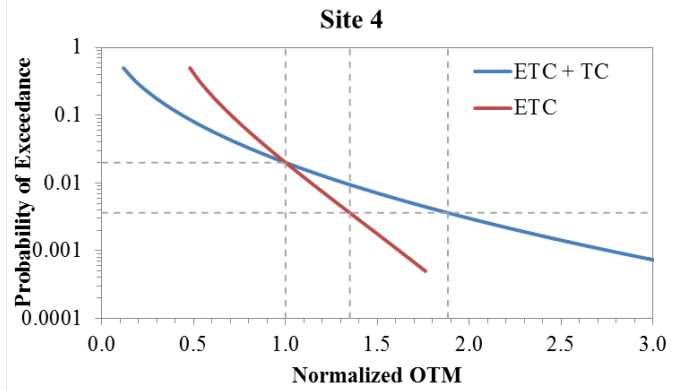
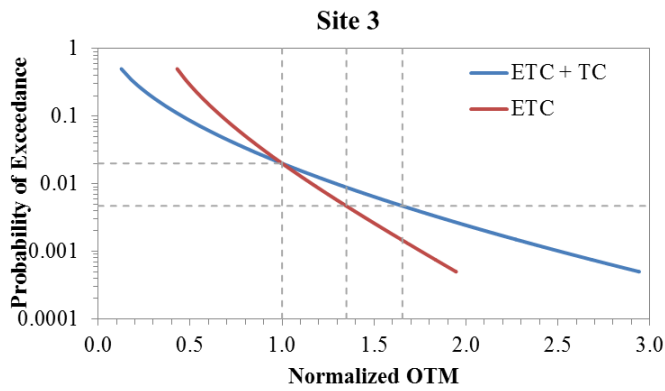
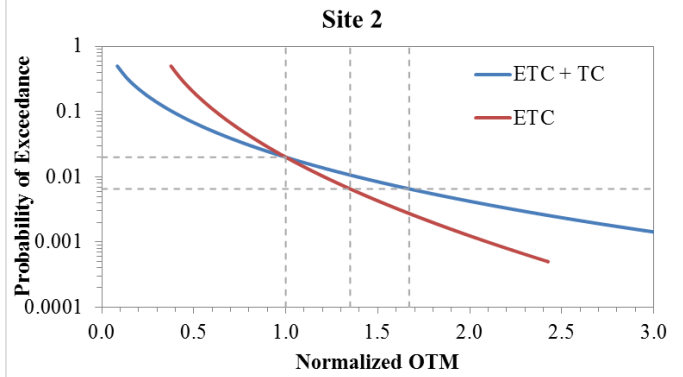
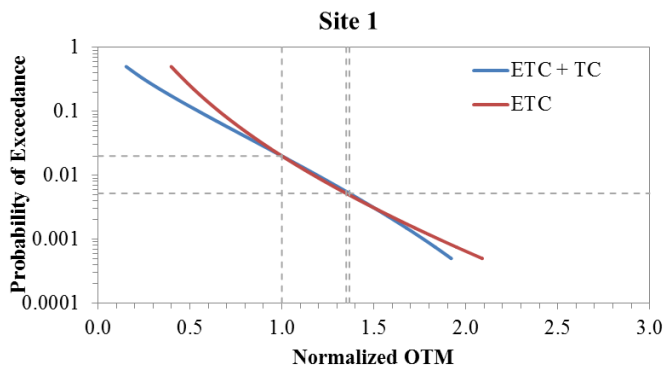


Figure 33 Normalized Base OTM Exceedance Curve for All Seven Sites

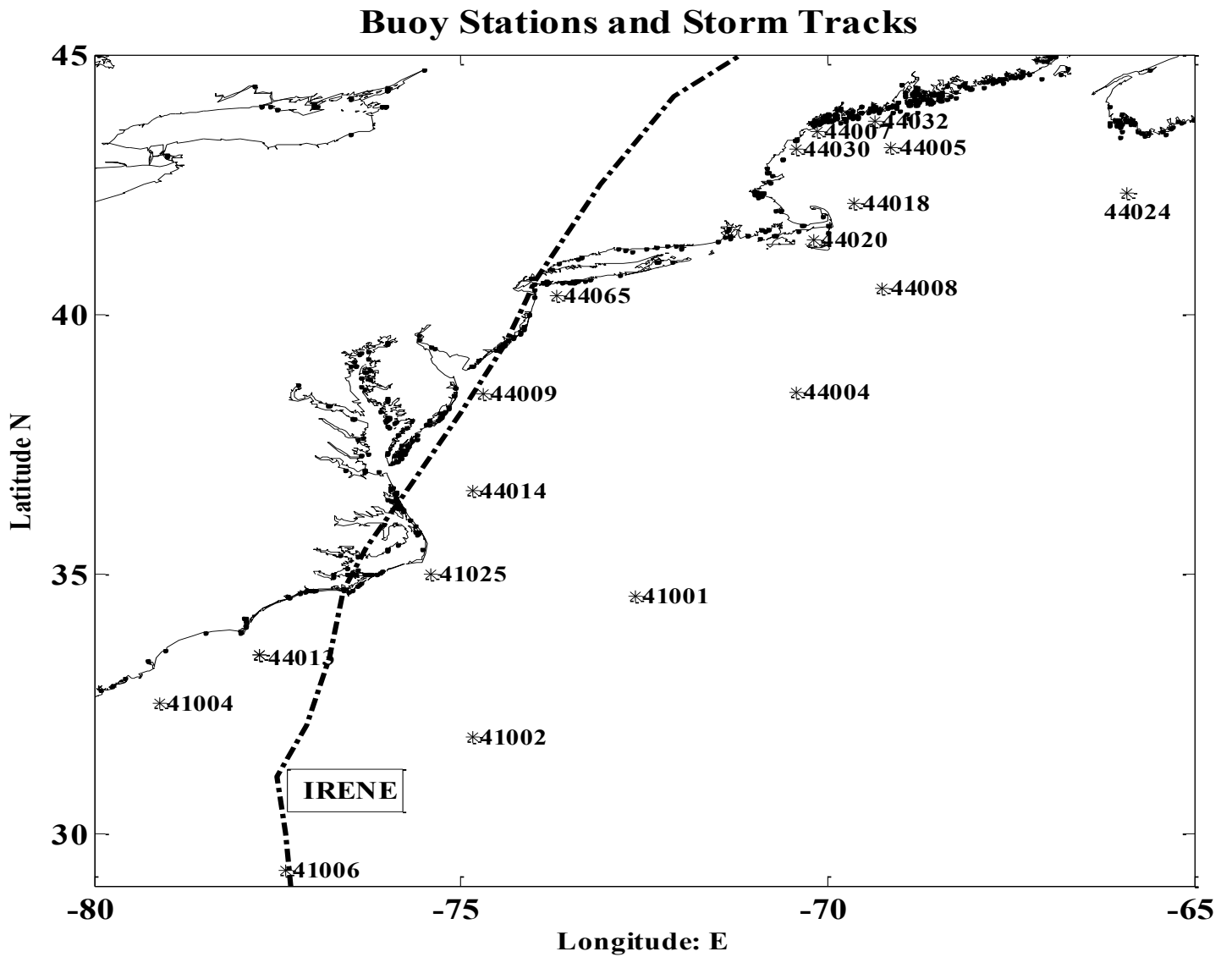
6.5. DISCUSSION OF RESULTS

As seen above, the two “end member” sites along the U.S. Eastern Seaboard, specifically Savannah to the south and Maine to the north, are at variance with the other five sites. The disparities can be explained both phenomenologically and statistically.

The Georgia site has experienced very few Extra-Tropical Cyclones as it is south of the principal region of ETC formation, intensification, re-intensification, and passage. While the entirety of the U.S. Eastern Seaboard has experienced ETC passages, the principal region essentially begins in Charleston SC and grows to the north along the seaboard to Cape Cod MA, where it veers to the northeast towards Europe. So Savannah is an ETC outlier and the statistics of the frequency of occurrence are very weak relative the other sites. The site is not sheltered by basin geography as is the Gulf of Maine site. Recognizing the site as an end member, the results for the Georgia site were found to be within anticipated limits and a load factor calculated.

Alternatively, the Maine site has had very few Tropical Cyclone realizations. So the statistics of those passages are very weak. Moreover the Maine site, within the Gulf of Maine, is at much deeper, greater depths than the other six sites, which changes the wave amplitude signatures significantly. The GOM site is also sheltered by its geography and thus even the ETC realizations are different than those of sites two through six. The fetch and duration of fetch associated with ETC passages are very different as passing ETCs are picked up by the Jet stream and moved towards the northeastern North Atlantic Ocean Basin towards Europe.

Appendix A buoy stations and storm tracks



Buoy stations used in the verification (for both TC IRENE (2011) and ETC 1993 winter storm) and the path of TC IRENE (2011)'s storm center.

Appendix B. Acronyms

BOEM (Bureau of Ocean Energy Management)
BSEE (Bureau of Safety and Environmental Enforcement)
CCU (Coastal Carolina University)
ETC (Extra Tropical Cyclone)
HPC (High Performance Computation)
IBTrACS (International Best Track Archive for Climate Stewardship)
MSLP (Mean Sea Level Pressure)
NARR (North American Regional Reanalysis)
NOAA (National Oceanic & Atmospheric Administration)
NDBC (National Data Buoy Center)
NESDIS (National Environmental Space & Data Information Service)
NOS (National Ocean Service)
NREL (National Environmental Renewable Energy Laboratory)
WEA (Wind Energy Areas)
BSEE (Bureau of Safety and Environmental Enforcement)
ETP (Emerging Technology Program)
ROMS (Regional Ocean Modeling System)
SWAN (Simulating Wave Nearshore)
SS (Saffir – Simpson Hurricane Category Scale)
TC (Tropical Cyclones)
US (United States)
WRF (Weather Research and Forecast)
WMO (World Meteorological Organization)
XSEDE (Extreme Science and Engineering Discovery Environment)